

H-Aggregated Form II Spherulite of Poly(3-butylthiophene) Grown from Solution

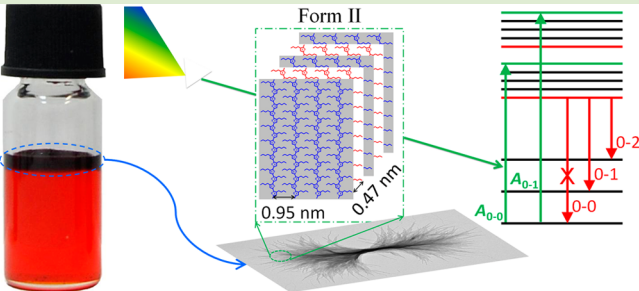
Yunpeng Qu,^{†,‡,§} Qing Su,^{†,‡} Sijun Li,^{†,‡,§} Guanghao Lu,^{†,‡,§} Xun Zhou,^{†,‡,§} Jidong Zhang,[‡] Zhaobin Chen,[†] and Xiaoni Yang^{*,†,‡}

[†]Polymer Composites Engineering Laboratory and [‡]State Key Laboratory of Polymer Physics and Chemistry, Changchun Institute of Applied Chemistry, Chinese Academy of Sciences, 5625 Renmin Street, Changchun 130022, P. R. China

[§]University of Chinese Academy of Sciences, Beijing 100049, P. R. China

S Supporting Information

ABSTRACT: New large-size poly(3-butylthiophene) (P3BT) spherulites are obtained by solution aging. These P3BT spherulites are composed of nanoribbons, and the P3BT molecules arrange into Form II structure with a backbone π -stacking distance of 0.47 nm. P3BT lamellae adopt “flat-on” orientation at the edge of the spherulite, and the spherulite preferentially grows along the π - π stacking direction. These spherulites could be obtained in bulk solution or at the top or bottom of the solution, depending on the competition of gravity and Brownian motion. Temperature-dependent photoluminescence spectra demonstrate that the polymer chains are arranged in H-aggregation model. The 0–0 transition in UV–visible absorption spectra blue shifts from 2.03 eV (610 nm, Form I) to 2.11 eV (589 nm, Form II). These results provide a further understanding of the crystallization and photophysical properties of poly(3-alkylthiophene) (P3AT), and the preparation method of large size and pure P3AT spherulites shows potential in applications of organic electronics.



Regioregular poly(3-alkylthiophene) (P3AT) is a classical semicrystalline conjugated polymer, which is intensively studied in the areas of thin film transistors,¹ polymer solar cells,^{2–4} etc. Since polythiophene was first reported in 1980,^{5,6} its polymorphic properties, such as intercalation of the alkyl side chains,⁷ π -stacking distance,⁸ tilt of the backbone,⁹ lamella orientation,⁸ growth direction,¹⁰ and crystal morphology (whisker,¹¹ spherulite,^{8,12,13} single crystal,^{14,15} and nanoribbon¹⁶), have continued to be the hot topic in academic society due to the importance in understanding and tailoring the electrical properties.¹⁷ The polymorphic behavior is governed by the molecule characteristics such as molecular weight (M_w),^{18–20} head-to-tail (HT) region-regularity,¹ polydispersity (PDI),^{20,21} and processing conditions such as pressure,²² crystallization temperature,²³ self-seeding,¹⁵ and post-treatment methods.^{7,8,10,13,14}

Of all the characteristics of crystal structures, π -stacking distance and conjugation length are the most important ones since charge carrier mobility in semicrystalline conjugated polymers is dominated by a charge-hopping transport mechanism.^{24–26} The influence of crystal structure on electrical properties could be reflected in optical spectroscopy. Previous photophysical studies were mainly focused on Form I crystals of poly(3-hexylthiophene) (P3HT) with a π - π stacking distance of 0.38 nm.²⁶ The polymer chains usually face-to-face stack into H-aggregates, in which, for example, the 0–0 transition is attenuated due to its forbidden nature. Recently,

Grey and Spano et al. reported that P3HT nanofibers self-assembled in toluene exhibit photophysical behavior of J-aggregates where, for instance, the 0–0 transition is enhanced relative to the 0–1 sideband.^{27,28} In this work, we dissolve poly(3-butylthiophene) (P3BT) in organic solvents and obtained a totally new P3BT spherulite composed of nanoribbons. In this P3BT spherulite, it is found for the first time that the P3BT molecular chains are arranged in H-aggregated Form II spherulite with π - π stacking distance of 0.47 nm, and the lamellae take different orientations at different positions of the spherulite. This Form II P3BT crystal shows new optical properties, for example, blue shift of the 0–0 transition in UV–visible (UV–vis) absorption spectra. In addition, an interesting finding is that the spherulites could be controlled to float on the top or precipitate at the bottom of the solutions by varying aging time and the solvent.

Figure 1(a) shows the transmission electron microscopy (TEM) image of bundle-like P3BT spherulite obtained from *o*-dichlorobenzene (ODCB) solution which has been aged at room temperature for 5 days. The spherulite is composed of nanoribbons with a maximum width of ca. 200 nm, which is different from that of the previously reported poly(3-dodecylthiophene) (P3DDT)¹² and P3BT spherulites.^{8,13}

Received: August 18, 2012

Accepted: October 15, 2012

Published: October 17, 2012

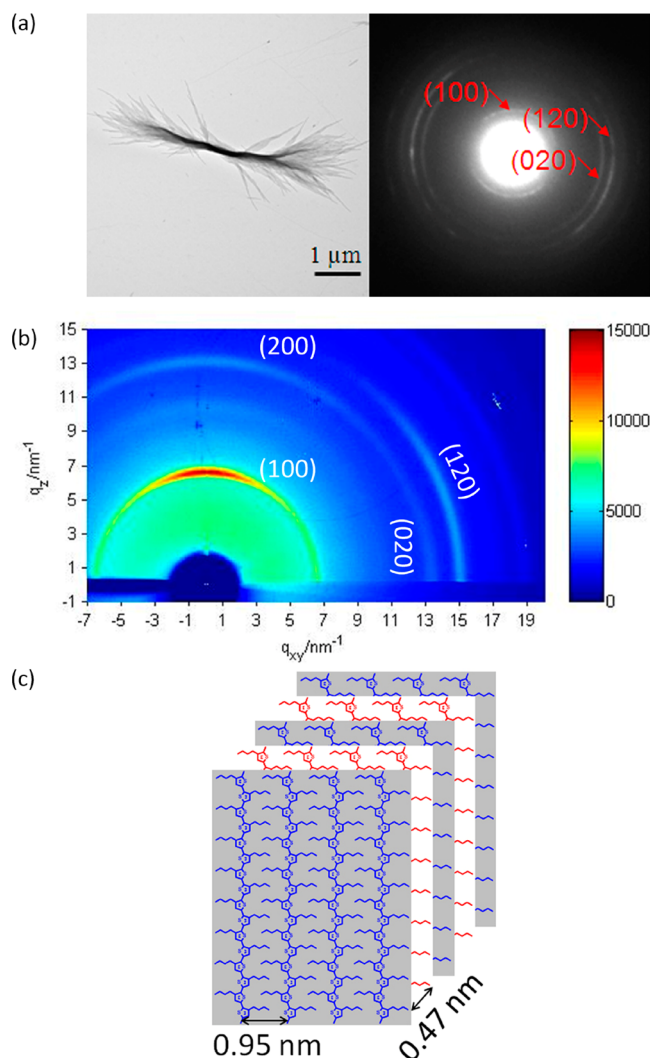


Figure 1. (a) Left, TEM image of P3BT spherulite grown from ODCB solution (5 mg/mL) after aging at room temperature for 5 days. Right, corresponding SAED pattern. (b) 2D-GIXRD pattern of P3BT Form II film. (c) Schematic polymer chain arrangement in Form II crystal.

composed of nanowhiskers. Nanoribbons have been found in P3HT,^{16,29} but they are separated from each other without further assembly. The selected-area electron diffraction (SAED) patterns (Figure 1(a) right) and two-dimensional grazing-incidence X-ray diffraction (2D-GIXRD) patterns (Figure 1(b)) of the spherulites show that the crystal structure could be attributed to P3BT Form II,^{8,13} which was first found by our group but under different preparation conditions. The d -spacing of the (100) plane is 0.95 nm ($q = 6.58 \text{ nm}^{-1}$), and the π - π stacking distance is 0.47 nm ($q = 13.3 \text{ nm}^{-1}$) (see Figure 1(c)).

Lamella orientation is one of the crucial parameters governing the performance of organic electronics. Considering the penetrating ability of the electronic beam (100–200 nm), the SAED pattern (Figure 1(a)) could be only contributed by the thin edge of the spherulite with light-gray color (the thickness of the dark middle part is around 1 μm). The pattern indicates that in the edge region the nanoribbons preferentially grow along the π - π stacking direction, and the lamellae take flat-on orientations in which the P3BT backbones adopt perpendicular alignment to the substrate. However, as to the film, which is composed of numerous spherulites, the lamellae

orientation is different. The 2D-GIXRD patterns in Figure 1(b), and corresponding polar coordinate and (100) intensity (Figure S-1, Supporting Information), show that the maximum intensity of the (100) arc exists at ca. 90° , which suggests that the lamellae in the whole film mainly take edge-on orientations with the backbones parallel to the substrate. The difference in lamella orientation partly suggests that the lamellae in the middle part of the spherulites, which could not be penetrated by electronic beam but by X-ray, might take edge-on orientation. Subsequently, the lamellae might gradually tilt with the growth of the spherulites and eventually achieve a flat-on orientation in the edge of the spherulite.

An interesting growth process of P3BT Form II spherulites in ODCB solution was observed as shown in Figure 2. At zero

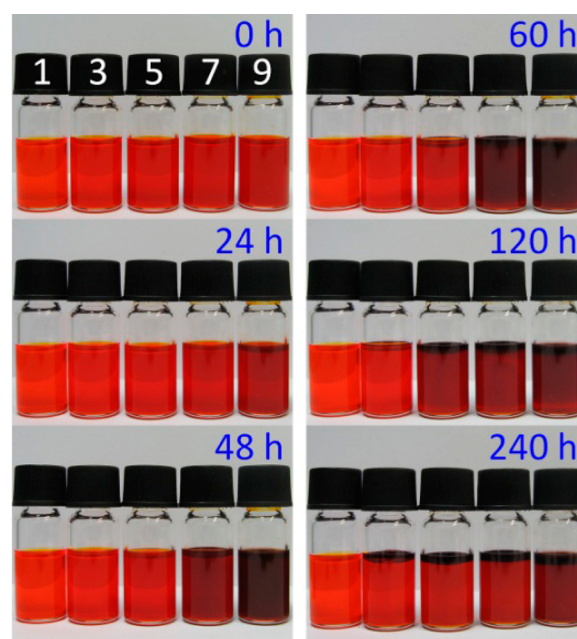


Figure 2. Aging process of the P3BT/ODCB solutions at concentrations of 1, 3, 5, 7, and 9 mg/mL (from left to right).

time point, all freshly prepared solutions show a transparent orange color. With the aging time elapsing, the solutions with the concentration of 5, 7, and 9 mg/mL get dark, and at the end of this testing round (240 h), an obvious P3BT spherulite layer is formed at the top of the solution, which was already demonstrated in Form II as described above. The color change of the solution of 3 mg/mL is not apparent; however, the layer could still be formed. In contrast, the solution with 1 mg/mL keeps transparent orange color without the formation of P3BT spherulites due to its low concentration. The morphologies of the P3BT spherulites formed at the top of and in the ODCB solution (9 mg/mL) are examined by an optical microscope (OM), as shown in Figure 3. From this figure it can be seen that P3BT forms two shapes of spherulites: one of them is bundle-like spherulites formed in the solution with main length of ca. 4–5 μm (Figure 3(a)), which is consistent in shape and size with the TEM observation (Figure 1(a)); the other one is bead-like spherulites formed at the top of the solution with a main diameter of 13–14 μm (Figure 3(b)), which is also well coincident with the TEM image shown in Figure S-2 (Supporting Information). It is believed that the bigger bead-

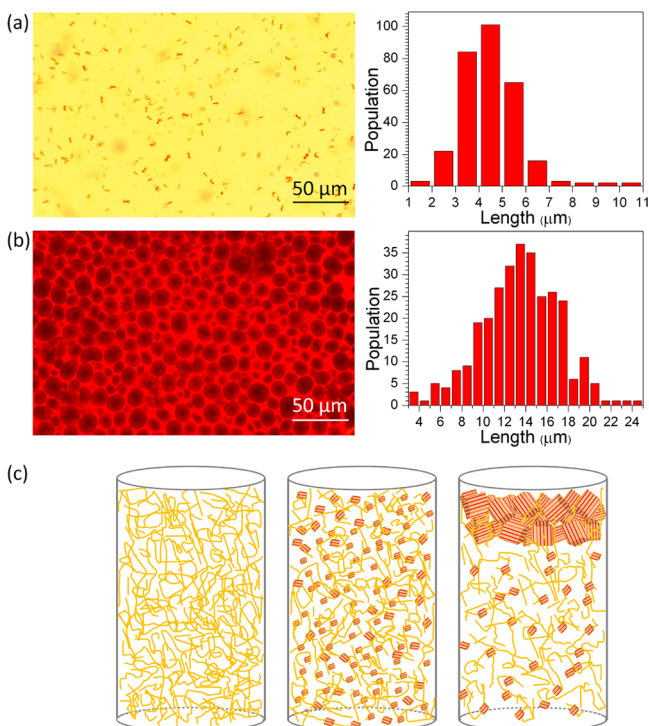


Figure 3. OM images and corresponding size distributions of P3BT Form II spherulites aged in ODCB (9 mg/mL) for 90 days. (a) Sampled from the bulk solution and (b) sampled from the top of the solution. (c) Illustration for the growth and distribution of P3BT Form II spherulites in ODCB solution.

like spherulites are grown from the small bundle-like spherulites with the prolonged aging time.

The P3BT Form II spherulites could be formed in other organic solvents such as *p*-xylene, toluene, and chlorobenzene (CB), and the same spherulite morphologies and similar layering phenomena in solution during aging are also observed (Figure S-3, Supporting Information). The difference is that the P3BT Form II spherulite layer is at the top of the ODCB solution and at the bottom of the latter three organic solvent solutions. The layering characteristic has never been reported in the literature for P3AT solutions in organic solvents. We speculate that the situations in organic solvent solution the P3BT Form II spherulites will depend on two factors: gravity and Brownian motion. For micrometer size particles, it could be characterized by Pelet number (Pe): $Pe = \tau_d / \tau_s = (\sigma^2 / D) / (\sigma / V_s)$, in which τ_d is the time it takes a particle to diffuse its own diameter; τ_s represents the time to sediment the same distance; σ is the diameter; D is the diffusion constant; and V_s is the sedimentation velocity. Using the Einstein relation for infinite dilution $D = k_B T / f$ and $V_s = m^* g / f$, with k_B the Boltzmann constant, T the kelvin temperature, f the friction factor, and m^* the particle buoyant mass, we obtained $Pe = m^* g \sigma / k_B T$, which is related only to the buoyant mass m^* and diameter σ of the particles.^{30,31} $Pe = 1$ is the dividing point between homogeneous suspension ($Pe < 1$) and the layering system ($Pe > 1$).^{30,31} It can be seen that a size increase in spherulites will result in higher m^* and σ values and thus Pe value, which is of benefit for the formation of the layering system. In our case, the Pe values of the bead-like spherulites estimated from the equation are far higher than 1 for all organic solvents (ODCB, *p*-xylene, toluene, and CB); therefore, layered solutions of P3BT Form II spherulites were obtained. For ODCB solution,

the layer of P3BT bead-like spherulite is at the top due to its lower density (about 1.2 g/cm³)³² compared to the ODCB solvent (1.33 g/cm³), while the higher density relative to toluene (0.87 g/cm³), *p*-xylene (0.88 g/cm³), and CB (1.11 g/cm³) leads to the formation of the P3BT spherulite layer at the bottom of the corresponding solutions. As for the bundle-like P3BT spherulites staying in the bulk solutions, the Brownian motion is the dominant factor due to the smaller size of the spherulites (average length ca. 4–5 μm), which prevents the spherulites from precipitation and buoying. The schematic spherulite growth process in ODCB solution is shown in Figure 3(c) as a typical example. At 0 h, the polymer chains are coil-like, and the solution shows a transparent orange appearance. Upon aging, the polymer chains gradually aggregate to form tiny bundle-like spherulites, and the solution turns darker (refer to sample solutions aged for 48 and 60 h in Figure 2). When the spherulites grow bigger, the influence of gravity becomes stronger than Brownian motion, which makes the spherulite move upward to the top. This process results in the decrease in the amount of P3BT in bulk solution and thus the lighter color (see sample solutions aged for 120 and 240 h in Figure 2). This layering behavior provides an attractive method to fabricate high-crystallinity materials for the studies on organic electronics and large-size spherulites for microfabrication.^{33,34}

As a new form of P3BT crystals, P3BT Form II spherulites exhibit different optical properties both in solution and in solid thin film compared with Form I, as shown in Figure 4. The

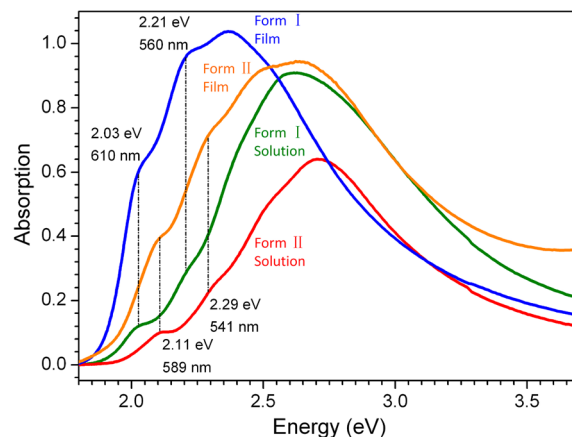


Figure 4. UV-vis absorption spectra of P3BT Form I whiskers in chloroform (CHCl₃) solution and Form II spherulites in ODCB solution and solid films cast from corresponding solutions.

Form II ODCB solution shows peaks at ca. 2.11 eV (589 nm) and ca. 2.29 eV (541 nm), which are attributed to the spherulites in the solution, since the well-dissolved P3AT solutions normally show a single absorption peak at ca. 460 nm.^{35,36} Form II film also shows two absorption peaks at the same positions, indicating that no solvatochromism,³⁷ which is based on spherulite–solvent interactions, exists in this system. Compared with Form II, the P3BT Form I nanowhiskers commonly show peaks at ca. 2.03 eV (610 nm) and ca. 2.21 eV (560 nm), both in solution and in solid film.^{38,39} The blue shift in the absorptions of the Form II crystals indicates the change of the electronic structures, which should be correlated with a decrease in polymer chain conjugation length with respect to Form I.^{23,26,32,40} The conjugation length of Form II is 20–30 Å (i.e., about 6 monomer units) according to the modeling

conducted by Meille et al.,³² which is much shorter than the one of Form I. A weak exciton coupling regime is expected in Form II, and the Form II absorption peaks at 2.11 and 2.29 eV could be ascribed to 0–0 and 0–1 transitions. The temperature-dependent photoluminescence (PL) spectra of P3BT Form II crystal films are shown in Figure 5(a). At 12 K, two

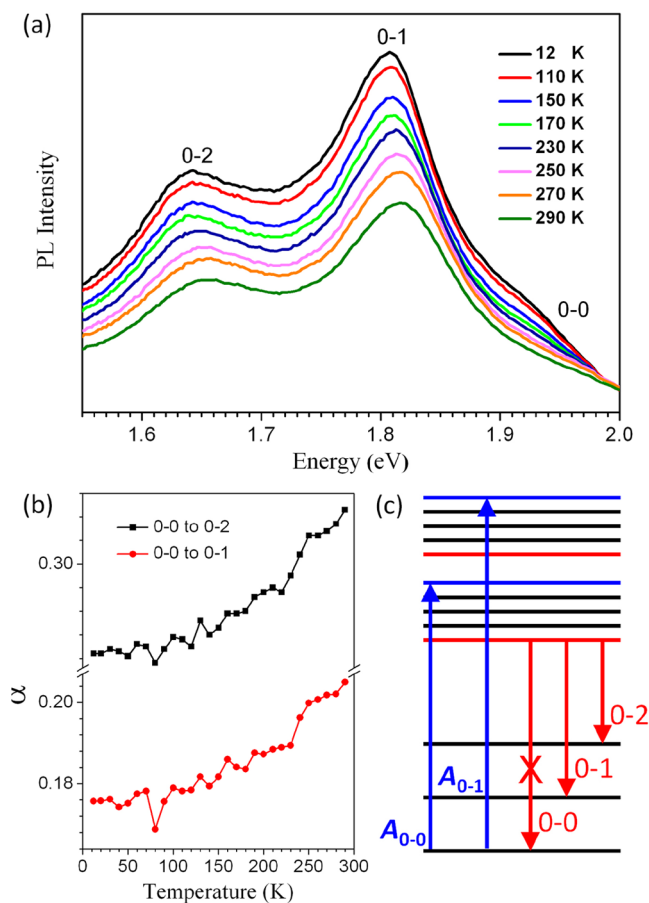


Figure 5. (a) PL spectra of P3BT Form II crystal films at various temperatures. (b) Variation of intensity ratios (α) of emission peaks with temperature. (c) Energy levels for a weakly coupled H-aggregate.

peaks are clearly observed at 1.81 eV (686 nm) and 1.64 eV (755 nm), which are assigned to 0–1 and 0–2 transitions, respectively. Three points in the spectra should be highlighted. First, no obvious 0–0 transition was observed. Second, on increasing temperature, 0–1 transition moves toward the higher-energy region from 1.80 eV (687 nm) to 1.82 eV (680 nm). Finally, the intensity ratios (α) of the emission peaks of 0–0 to 0–1 and 0–0 to 0–2, shown in Figure 5(b), gradually increase with increasing temperature. All these characteristics are in agreement with the spectral signatures of H aggregates,⁴¹ and the corresponding schematic energy levels are shown in Figure 5(c). The free exciton bandwidth (W) of P3BT Form II crystals was calculated from the intensities of 0–0 and 0–1 absorption peaks according to the following equation^{42–45}

$$\frac{A_{0-0}}{A_{0-1}} \approx \left(\frac{1 - 0.24W/E_p}{1 + 0.073W/E_p} \right)^2$$

E_p is the phonon energy of the main oscillator coupled to the electronic transition, which is assumed to be dominated by C=C symmetric stretching here, and could be obtained by a

Raman study (Figure S-4, Supporting Information) showing two peaks at 1378 cm^{-1} (0.17 eV) and 1445 cm^{-1} (0.18 eV). This spectrum is very similar to the Form I crystals, and these two peaks can be assigned to the ring C–C stretching and the symmetric C=C stretching, respectively.⁴⁶ The free exciton bandwidth is calculated to be ca. 158 meV, which is higher than that of P3HT Form I films obtained from solutions such as chloroform (120 meV), thiophene (ca. 90 meV), and isodurene (20 meV)^{44,45} and higher than that of the P3BT Form I film obtained from chloroform solution in this work (ca. 123 meV). This relatively higher free exciton bandwidth is probably related to the lower conjugation length.^{23,26,32,40} Further photophysical studies such as fluorescence lifetimes, quantum yields, and fluorescence quenching in the presence of fullerene are currently in process.

In this study, highly crystallized new Form II P3BT spherulites with large size (13–14 μm in diameter) are obtained by the simple method of organic solvent solution aging. These P3BT spherulites are composed of nanoribbons, and P3BT molecules in this form have the arrangement of (100) d -spacing of 0.95 nm and π -stacking distance of 0.47 nm. 2D-GIXRD analysis reveals that the P3BT lamellae adopt different orientations in the spherulites: “flat-on” orientation at the edge and “edge-on” orientation at the middle part of the spherulites. The UV-vis spectra show a blue shift of 0–0 transition from ca. 2.03 eV (610 nm, Form I) to ca. 2.11 eV (589 nm, Form II) due to the changes in conjugation length. The temperature-dependent PL spectra demonstrated that the P3BT molecular chains are arranged in a H-aggregation model. The development of this simple method and the finding of the new form P3BT spherulites are essentially significant for study on the photophysical properties of P3AT-based conjugated polymers and fabrication of high performance electronic devices.

■ ASSOCIATED CONTENT

📄 Supporting Information

Experimental methods, polar-coordinate 2D-GIXRD patterns, additional TEM image of P3BT spherulite, pictures for P3BT solutions in *p*-xylene, toluene, and CB, and Raman spectrum. This material is available free of charge via the Internet at <http://pubs.acs.org>.

■ AUTHOR INFORMATION

Corresponding Author

*E-mail: xnyang@ciac.jl.cn.

Notes

The authors declare no competing financial interest.

■ ACKNOWLEDGMENTS

This work was funded by the National Natural Science Foundation of China (20874100, 20990233), Hi-Tech Research and Development Program (863) of China (2011AA050524), and Solar Energy Initiative (KGCX2-YW-399 + 9) of the Chinese Academy of Sciences. X.Y. would also like to thank the Fund for Distinguished Young Scholars (20925415) and the Fund for Creative Research Groups (50921062) of NSFC for financial support. The authors acknowledge Dr. Frank C. Spano for his valuable discussions about the relationship between crystal structure and photophysical properties. Mr. Jinfeng Li (Department of Physics, University of California, Irvine) is acknowledged for his kind

help in fitting the UV–vis spectra and programming the software for 2D-GIXRD analysis. The synchrotron-based 2D-GIXRD measurement was supported by Shanghai Synchrotron Radiation Facility.

REFERENCES

- (1) Sirringhaus, H.; Brown, P. J.; Friend, R. H.; Nielsen, M. M.; Bechgaard, K.; Langeveld-Voss, B. M. W.; Spiering, A. J. H.; Janssen, R. A. J.; Meijer, E. W.; Herwig, P.; de Leeuw, D. M. *Nature* **1999**, *401* (6754), 685–688.
- (2) Yang, X. N.; Loos, J.; Veenstra, S. C.; Verhees, W. J. H.; Wienk, M. M.; Kroon, J. M.; Michels, M. A. J.; Janssen, R. A. J. *Nano Lett.* **2005**, *5* (4), 579–583.
- (3) He, X. M.; Gao, F.; Tu, G. L.; Hasko, D.; Huttner, S.; Steiner, U.; Greenham, N. C.; Friend, R. H.; Huck, W. T. S. *Nano Lett.* **2010**, *10* (4), 1302–1307.
- (4) Padinger, F.; Rittberger, R. S.; Sariciftci, N. S. *Adv. Funct. Mater.* **2003**, *13* (1), 85–88.
- (5) Yamamoto, T.; Sanechika, K.; Yamamoto, A. J. *Polym. Sci., Part C: Polym. Lett.* **1980**, *18* (1), 9–12.
- (6) Lin, J. W. P.; Dudek, L. P. J. *Polym. Sci., Part A: Polym. Chem.* **1980**, *18* (9), 2869–2873.
- (7) Prosa, T. J.; Winokur, M. J.; McCullough, R. D. *Macromolecules* **1996**, *29* (10), 3654–3656.
- (8) Lu, G. H.; Li, L. G.; Yang, X. N. *Adv. Mater.* **2007**, *19* (21), 3594–3598.
- (9) DeLongchamp, D. M.; Kline, R. J.; Lin, E. K.; Fischer, D. A.; Richter, L. J.; Lucas, L. A.; Heeney, M.; McCulloch, I.; Northrup, J. E. *Adv. Mater.* **2007**, *19* (6), 833–837.
- (10) Xiao, X. L.; Wang, Z. B.; Hu, Z. J.; He, T. B. *J. Phys. Chem. B* **2010**, *114* (22), 7452–7460.
- (11) Ihn, K. J.; Moulton, J.; Smith, P. J. *Polym. Sci., Part B: Polym. Phys.* **1993**, *31* (6), 735–742.
- (12) Wang, W.; Toh, K. C.; Tji, C. W. *Macromol. Chem. Phys.* **2004**, *205* (9), 1269–1273.
- (13) Lu, G. H.; Li, L. G.; Yang, X. N. *Macromolecules* **2008**, *41* (6), 2062–2070.
- (14) Ma, Z. Y.; Geng, Y. H.; Yan, D. H. *Polymer* **2007**, *48* (1), 31–34.
- (15) Kim, D. H.; Han, J. T.; Park, Y. D.; Jang, Y.; Cho, J. H.; Hwang, M.; Cho, K. *Adv. Mater.* **2006**, *18* (6), 719–723.
- (16) Liu, J. H.; Arif, M.; Zou, J. H.; Khondaker, S. I.; Zhai, L. *Macromolecules* **2009**, *42* (24), 9390–9393.
- (17) Yamamoto, T. *NPG Asia Mater.* **2010**, *2*, 54–60.
- (18) Zen, A.; Saphiannikova, M.; Neher, D.; Grenzer, J.; Grigorian, S.; Pietsch, U.; Asawapirom, U.; Janietz, S.; Scherf, U.; Lieberwirth, I.; Wegner, G. *Macromolecules* **2006**, *39* (6), 2162–2171.
- (19) Brinkmann, M.; Rannou, P. *Adv. Funct. Mater.* **2007**, *17* (1), 101–108.
- (20) Hiorns, R. C.; De Bettignies, R.; Leroy, J.; Bailly, S.; Firon, M.; Sentein, C.; Khoukh, A.; Preud'homme, H.; Dagon-Lartigau, C. *Adv. Funct. Mater.* **2006**, *16* (17), 2263–2273.
- (21) Kohn, P.; Huettner, S.; Komber, H.; Senkovskyy, V.; Tkachov, R.; Kiriya, A.; Friend, R. H.; Steiner, U.; Huck, W. T. S.; Sommer, J.-U.; Sommer, M. *J. Am. Chem. Soc.* **2012**, *134* (10), 4790–4805.
- (22) Muller, C.; Zhigadlo, N. D.; Kumar, A.; Baklar, M. A.; Karpinski, J.; Smith, P.; Kreouzis, T.; Stingelin, N. *Macromolecules* **2011**, *44* (6), 1221–1225.
- (23) Arosio, P.; Moreno, M.; Famulari, A.; Raos, G.; Catellani, M.; Meille, S. V. *Chem. Mater.* **2009**, *21* (1), 78–87.
- (24) Chen, Z. H.; Muller, P.; Swager, T. M. *Org. Lett.* **2006**, *8* (2), 273–276.
- (25) Forrest, S. R. *Chem. Rev.* **1997**, *97* (6), 1793–1896.
- (26) Salleo, A.; Kline, R. J.; DeLongchamp, D. M.; Chabinyc, M. L. *Adv. Mater.* **2010**, *22* (34), 3812–3838.
- (27) Niles, E. T.; Roehling, J. D.; Yamagata, H.; Wise, A. J.; Spano, F. C.; Moulé, A. J.; Grey, J. K. *J. Phys. Chem. Lett.* **2012**, *3* (2), 259–263.
- (28) Yamagata, H.; Spano, F. C. *J. Chem. Phys.* **2012**, *136* (18), 184901.
- (29) Arif, M.; Liu, J. H.; Zhai, L.; Khondaker, S. I. *Appl. Phys. Lett.* **2010**, *96* (24), 243304.
- (30) Wijnhoven, J. E. G. J.; van't Zand, D. D.; van der Beek, D.; Lekkerkerker, H. N. W. *Langmuir* **2005**, *21* (23), 10422–10427.
- (31) Wysocki, A.; Royall, C. P.; Winkler, R. G.; Gompper, G.; Tanaka, H.; van Blaaderen, A.; Lowen, H. *Soft Matter* **2009**, *5* (7), 1340–1344.
- (32) Buono, A.; Son, N. H.; Raos, G.; Gila, L.; Cominetti, A.; Catellani, M.; Meille, S. V. *Macromolecules* **2010**, 6772–6781.
- (33) Loos, J.; Sourty, E.; Lu, K.; Freitag, B.; Tang, D.; Wall, D. *Nano Lett.* **2009**, *9* (4), 1704–1708.
- (34) Kawase, N.; Kato, M.; Nishioka, H.; Jinnai, H. *Ultramicroscopy* **2007**, *107* (1), 8–15.
- (35) Zhou, X.; Yang, X. N. *Carbon* **2012**, *50* (12), 4566–4572.
- (36) Li, L. G.; Lu, G. H.; Yang, X. N. *J. Mater. Chem.* **2008**, *18* (17), 1984–1990.
- (37) Würthner, F.; Archetti, G.; Schmidt, R.; Kuball, H.-G. *Angew. Chem., Int. Ed.* **2008**, *47* (24), 4529–4532.
- (38) Qu, Y. P.; Li, L. G.; Lu, G. H.; Zhou, X.; Su, Q.; Xu, W. T.; Li, S. J.; Zhang, J. D.; Yang, X. N. *Polym. Chem.* **2012**, DOI: 10.1039/C2PY20400B.
- (39) Brown, P. J.; Thomas, D. S.; Kohler, A.; Wilson, J. S.; Kim, J. S.; Ramsdale, C. M.; Sirringhaus, H.; Friend, R. H. *Phys. Rev. B* **2003**, *67* (6), 064203.
- (40) Barford, W. J. *Chem. Phys.* **2007**, *126* (13), 134905.
- (41) Spano, F. C. *Acc. Chem. Res.* **2010**, *43* (3), 429–439.
- (42) Spano, F. C. *Chem. Phys.* **2006**, *325* (1), 22–35.
- (43) Spano, F. C. *J. Chem. Phys.* **2005**, *122* (23), 234701.
- (44) Clark, J.; Chang, J. F.; Spano, F. C.; Friend, R. H.; Silva, C. *Appl. Phys. Lett.* **2009**, *94* (16), 163306.
- (45) Clark, J.; Silva, C.; Friend, R. H.; Spano, F. C. *Phys. Rev. Lett.* **2007**, *98* (20), 206406.
- (46) Louarn, G.; Trznadel, M.; Buisson, J. P.; Laska, J.; Pron, A.; Lapkowski, M.; Lefrant, S. J. *Phys. Chem.* **1996**, *100* (30), 12532–12539.